Quasibound States in the Continuum in a Two Channel Quantum Wire with an Adatom

Hiroaki Nakamura*
Department of Simulation Science, National Institute for Fusion Science, Oroshi-cho, Toki, Gifu 509-5292, Japan

Naomichi Hatano†
Institute of Industrial Science, University of Tokyo, Komaba, Meguro, Tokyo 153-8505, Japan

Sterling Garmon and Tomio Petrosky
Center for Complex Quantum Systems, University of Texas at Austin, 1 University Station, C1609, Austin, Texas 78712, USA
(Received 2 August 2007; published 20 November 2007)

We report the prediction of quasibound states (resonant states with very long lifetimes) that occur in the eigenvalue continuum of propagating states for certain systems in which the continuum is formed by two overlapping energy bands. We illustrate this effect using a quantum wire system with two channels and an attached adatom. When the energy bands of the two channels overlap, a would-be bound state that lays just below the upper energy band is slightly destabilized by the lower energy band and thereby becomes a resonant state with a very long lifetime (a second such state lays above the lower energy band). Unlike the bound states in continuum predicted by von Neumann and Wigner, these states occur for a wide region of parameter space.

DOI: 10.1103/PhysRevLett.99.210404 PACS numbers: 03.65.Ge, 73.21.Hb, 73.20.At

Since the bound state in continuum (BIC) was first proposed in 1929 by von Neumann and Wigner [1], various researchers have reported its existence [2–10]. All studies agree that the phenomenon can only occur at discrete points of parameter space (i.e., the BIC is a zero-measure effect).

We here report the existence of a *quasi*-bound state in continuum that exists over a wide region of parameter space (finite measure). By quasibound state, we mean a metastable state that decays on a very long time scale and appears to be a bound state in space. The quasibound state emerges when the system has an excited discrete state coupled to two overlapping energy bands with divergent singularities in the density of electronic states at the band edges (which are called van Hove singularities in the context of solid-state physics). If the excited state were coupled to only one energy band, a bound state would appear just outside the edge (due to the singularity) [11–13]. This would-be bound state is slightly destabilized by the second energy band, forming a quasibound state. The quasibound state in continuum may be useful to produce a high-energy semiconductor laser, because the energy difference between a bound state and a quasibound state in continuum can be much greater than the energy difference between two bound states.

We demonstrate this phenomenon with a two-channel quantum wire system with an adatom or a quantum dot. A quantum wire with a side-coupled dot has been fabricated [14] and analyzed [15], where the typical length scale (such as the distance between the wire and the dot) is on the order of μm and the typical energy scale (such as the hopping parameters t_h and g below) is on the order of 100 μeV. Our Hamiltonian is the tight-binding model on a ladder with the adatom, or the dot [Fig. 1(a)]:

$$\mathcal{H} = -\frac{t_h}{2}\sum_{y=1,2}\sum_{x=-\infty}^{\infty}(c^\dagger_{x+1,y}c_{x,y} + c^\dagger_{x,y}c_{x+1,y}) - t'_h\sum_{x=-\infty}^{\infty}(c^\dagger_{x,2}c_{x,1} + c^\dagger_{x,1}c_{x,2}) + g(d^\dagger c_{0,1} + c^\dagger_{0,1}d) + E_d d^\dagger d. \quad (1)$$

Here, $c_{x,y}$ are the annihilation operators of a spinless fermion at the site (x, y) with integer x $(-\infty < x < \infty)$ and $y = 1, 2$, whereas $d^\dagger$ and d represent an adatom attached to the (0, 1) site of the ladder. The first term of Eq. (1) gives the hopping matrix elements along the ladder, the second term the hopping elements across the ladder,

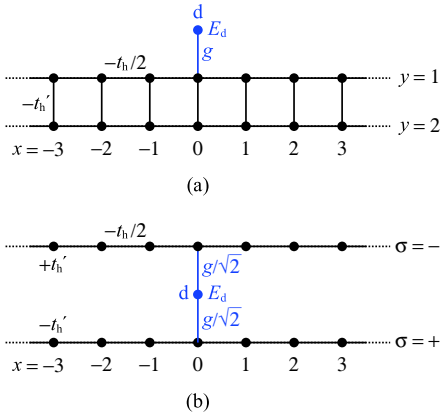

FIG. 1 (color online). (a) An adatom attached to a ladder. (b) After diagonalizing the ladder, the system is composed of an adatom coupled to two independent channels.

and the third term gives the hopping elements to and from the one-particle level of the adatom.

The ladder has two eigenmodes $c_{x,\pm} \equiv (c_{x,1} \pm c_{x,2})/\sqrt{2}$, which transform the Hamiltonian (1) to

$$\mathcal{H} = -\frac{t_h}{2}\sum_{\sigma=\pm}\sum_{x=-\infty}^{\infty}(c^\dagger_{x+1,\sigma}c_{x,\sigma} + c^\dagger_{x,\sigma}c_{x+1,\sigma}) - t'_h\sum_{\sigma=\pm}\sum_{x=\infty}^{\infty}\sigma c^\dagger_{x,\sigma}c_{x,\sigma} + \frac{g}{\sqrt{2}}\sum_{\sigma=\pm}(d^\dagger c_{0,\sigma} + c^\dagger_{0,\sigma}d) + E_d d^\dagger d, \quad (2)$$

see Fig. 1(b). The Fourier transform $c^\dagger_{k_\pm,\pm} = (2\pi)^{-1/2}\times\sum_{x=-\infty}^{\infty} e^{ik_\pm x}c^\dagger_{x,\pm}$ reveals that the system has two conduction channels with $-\pi \le k_\pm \le \pi$, each of which forms an energy band (a continuum)

$$\varepsilon_\pm(k_\pm) = -t_h\cos k_\pm \mp t'_h. \quad (3)$$

Two divergent van Hove singularities occur in the density of states at the edges of both bands [13]. The two bands overlap (with one of the singularities of one band embedded within the continuum of the other) whenever $|t'_h| < |t_h|$. The adatom level couples to both channels as can be seen in Eq. (2). We can also regard the Hamiltonian (2) as conducting electrons with spin σ on a tight-binding chain under a magnetic field proportional to t'_h.

In terms of the new operators $c^\dagger_{k_\pm,\pm}$, the Hamiltonian (2) takes the form of the coupled Friedrichs-Fano (Newns-Anderson) model Hamiltonian [16–19], which has been thoroughly studied. Using the standard argument for this model, we obtain the dispersion equation for this coupled system:

$$z - E_d - \frac{g^2}{2}\left[\frac{1}{\sqrt{(z+t'_h)^2 - t_h^2}} - \frac{1}{\sqrt{(z-t'_h)^2 - t_h^2}}\right] = 0. \quad (4)$$

This is equivalent to a twelfth order polynomial equation for z. The complex solutions of this equation correspond to the complex energy eigenvalues of the resonance states, with the decay rate given by the imaginary part.

We first focus on the numerical solution of this equation, using $t'_h = 0.345t_h$ and $g = 0.1t_h$ for our demonstration. The 12 eigenvalues for $E_d = 0.3t_h$ are listed in Table I, as an example.

Each discrete eigenvalue can be distinguished by its position on the complex K_+ surface, the complex K_- surface and the complex energy surface, where the three quantities are related by $E = -t_h\cos K_+ - t'_h = -t_h\cos K_- + t'_h$. The corresponding eigenfunction is given in the form

$$\begin{pmatrix}\Psi(x,1;t)\\ \Psi(x,2;t)\end{pmatrix} = e^{-iEt/\hbar}\left(A_+ e^{iK_+|x|}\begin{pmatrix}1\\1\end{pmatrix} + A_- e^{iK_-|x|}\begin{pmatrix}1\\-1\end{pmatrix}\right) \quad (5)$$

with appropriate constants $A_\pm$.

The complex energy surface is composed of four Riemann sheets. It is a physical requirement [20] that a resonant state decays in time but diverges in space. The resonant state, therefore, has a negative imaginary part for its energy and a negative imaginary part for one or both of the wave numbers K_+ and K_-. An eigenvalue in the upper K_+ plane and in the upper K_- plane is defined to lay on Riemann sheet I and is a complete bound state; the states $P1$ and $P2$ in Table I are such states. An eigenvalue in the lower K_+ plane and in the lower K_- plane is defined to lay on Riemann sheet IV and is a resonant state; the state $S1$ in Table I is such a state.

An eigenvalue in the lower K_+ plane but in the upper K_- plane is defined to lay on Riemann sheet II, while one in the upper K_+ plane but in the lower K_- plane is defined to lay on Riemann sheet III. The resonant states on these two sheets (states $Q2$, $Q4$, and $R2$ in Table I) are the main focus of the present Letter.

These states in sheets II and III are resonant states because they diverge in space due to the negative imaginary part of only one of the wave numbers; see Eq. (5).

TABLE I. The 12 discrete eigenvalues for $t'_h = 0.345t_h$, $g = 0.1t_h$ and $E_d = 0.3t_h$.

State	E/t_h	K_+	K_-	Riemann Sheet
$P1(0.3)$	1.345 011 52	3.141 592 65 + i1.115 932 56	3.14159265 + i0.00480148	I
$P2(0.3)$	−1.345 004 63	+i0.003 046 29	+i1.115 927 51	I
$Q1(0.3)$	1.345 011 36	3.141 592 65 − i1.115 932 45	3.141 592 65 + i0.004 767 87	II
$Q2(0.3)$	$-0.655\,013\,70 - i1.5093\times10^{-7}$	$1.255\,588\,88 - i1.5875\times10^{-7}$	$-0.000\,028\,82 + i0.005\,235\,34$	II
$Q3(0.3)$	$-0.655\,013\,70 + i1.5093\times10^{-7}$	$-1.255\,588\,88 - i1.5875\times10^{-7}$	$0.000\,028\,82 + i0.005\,235\,34$	II
$Q4(0.3)$	0.299 988 54 − i0.001 537 74	2.271 802 90 − i0.002 012 24	−1.525 769 70 + i0.001 539 30	II
$Q5(0.3)$	0.299 988 54 + i0.001 537 74	−2.271 802 90 − i0.002 012 24	1.525 769 70 + i0.001 539 30	II
$R1(0.3)$	−1.345 004 59	+i 0.003 032 73	−i 1.115 927 48	III
$R2(0.3)$	$0.655\,099\,06 - i2.9331\times10^{-6}$	−3.141 384 29 + i0.014 077 02	$1.886\,093\,55 - i3.0852\times10^{-6}$	III
$R3(0.3)$	$0.655\,099\,06 + i2.9331\times10^{-6}$	3.141 384 29 + i0.014 077 02	$-1.886\,093\,55 - i3.0852\times10^{-6}$	III
$S1(0.3)$	0.299 919 27 − i0.011 544 76	2.271 617 73 − i0.015 104 19	1.525 703 33 − i0.011 556 25	IV
$S2(0.3)$	0.299 919 27 + i0.011 544 76	−2.271 617 73 − i0.015 104 19	−1.525 703 33 − i0.0115 562 5	IV

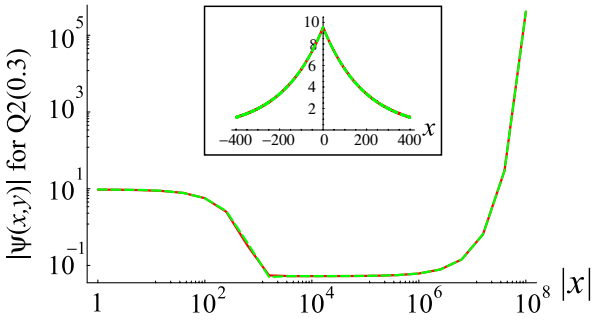

FIG. 2 (color online). The wave function modulus $|\psi(x, y)|$ of the state $Q2$ around the origin on the linear scale (inset) and away from the origin on the logarithmic scale. The plots for $y = 1$ (the upper leg) and $y = 2$ (the lower leg) are almost indiscernible. The parameters are set to $t_h' = 0.345t_h$, $g = 0.1t_h$, and $E_d = 0.3t_h$.

Some of them, however, diverge in space very slowly and decay in time very slowly (the latter is demonstrated in Table I). The state $Q2$, for example, *appears* to be a localized state around the x-axis origin and exponentially diverges only far away (Fig. 2).

Indeed, analytically solving the dispersion relation (4) by perturbation expansion in g, we find that the imaginary part of the energy of state $Q2$ is proportional to g^6 (extremely small for $g \ll 1$) due to the interaction between the divergent van Hove singularity in the upper energy band and the continuum of the lower band. Since the real part of the energy lays within the lower energy band, we refer to this state as a quasibound state in continuum (QBIC).

The quasibound state $Q2$ has the real part of the energy just below the lower edge of the upper energy band ε_-, which occurs at $-t_h + t_h' = -0.655t_h$ in the present case. If we had only the upper channel, this state would be a bound state (due to the van Hove singularity) [11–13]. In order to elucidate how the QBIC effect appears, we compare the above result to that obtained for the separate one-channel systems with the following new Hamiltonians with a structure similar to Eq. (2):

$$\mathcal{H}_\pm = -\frac{t_h}{2}\sum_{x=-\infty}^{\infty}(c_{x+1}^\dagger c_x + c_x^\dagger c_{x+1}) + \frac{g}{\sqrt{2}}(d^\dagger c_0 + c_0^\dagger d) + E_d d^\dagger d \mp t_h'. \quad (6)$$

Here we set the coupling between the site $x = 0$ and the adatom to $g/\sqrt{2}$ for quantitative comparison with the Hamiltonian (2). We have also added the energy offset $\mp t_h'$ so that the energy band of each Hamiltonian $\mathcal{H}_\pm$ may coincide with the energy bands $\varepsilon_\pm$ of the ladder system. The Hamiltonian $\mathcal{H}_-$ thus mimics the upper energy band ε_- of the $-$ channel of the ladder system, while the Hamiltonian $\mathcal{H}_+$ mimics the lower band ε_+.

The bound state below the lower band edge of the Hamiltonian $\mathcal{H}_-$ for $t_h' = 0.345t_h$, $g = 0.1t_h$ and $E_d = 0.3t_h$ has a pure real energy $E/t_h = -0.655\,013\,71$ and a pure imaginary wave number $K = i0.005\,235\,50$. This bound state of the one-channel system [Fig. 3(a)] indeed closely resembles the eigenvalue and the wave number K_- of state $Q2$ of the two-channel system (see Table I).

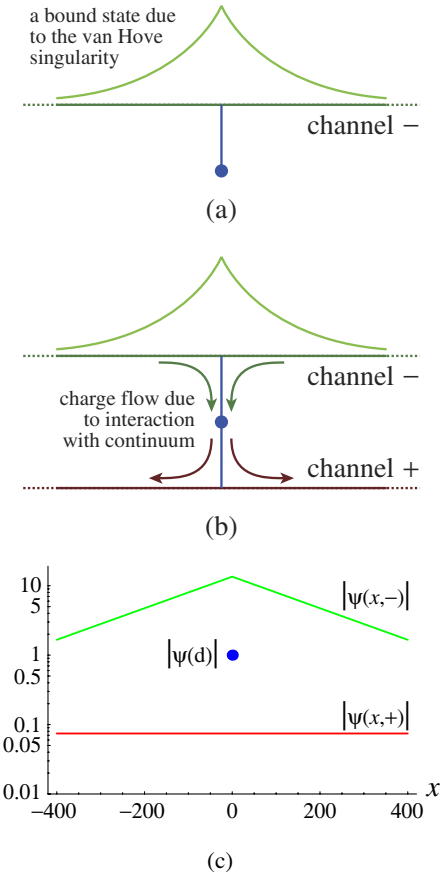

FIG. 3 (color online). (a) A schematic view of the strongly bound state (due to the van Hove singularity) of a one-channel system with the eigenvalue just below the lower band edge. (b) Some of the bound particles leak into the attached channel. (c) The eigenfunction of the state $Q2$ for $t_h' = 0.345t_h$, $g = 0.1t_h$ and $E_d = 0.3t_h$. The amplitude modulus of the $-$ channel, $|\psi(x, -)|$, that of the $+$ channel, $|\psi(x, +)|$, and that of the adatom, $|\psi(d)|$, are indicated.

When the second channel is attached to the one-channel system [Fig. 3(b)], the energy is inside the conduction band of the $+$ channel so that a portion of the bound particles outside the edge of the $-$ channel leak into the $+$ channel and escape to infinity. Notice $\mathrm{Re}K_- < 0$, while $\mathrm{Re}K_+ > 0$; the particles on the channel $-$ are pulled into the origin and then spring out into the $+$ channel. This leak makes the state $Q2$ a resonant state; it can be generally shown [20] that the imaginary part of the resonant eigenvalue arises due to the momentum flux escaping from the scattering potential.

The actual eigenfunction of the state $Q2$ is exemplified in Fig. 3(c). One can analytically show that the amplitude at the adatom $\psi(d)$ is order g smaller ($g = 0.1t_h$ in this

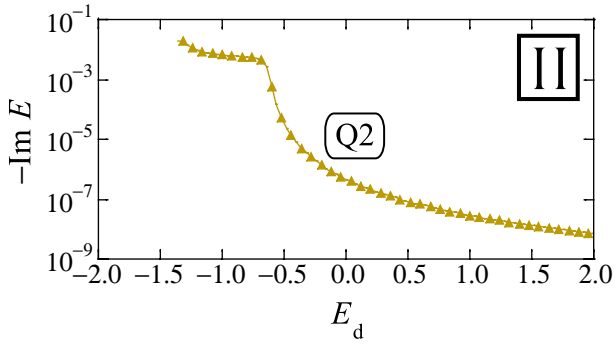

FIG. 4 (color online). The dependence of the imaginary part of the eigenvalues of the state $Q2$ on the one-particle level of the adatom E_d. The imaginary part vanishes for $E_d \lesssim -1.345t_h$. The parameters are set to $t_h' = 0.345t_h$ and $g = 0.1t_h$.

case) than the amplitude of $\psi(0, -)$ and the amplitude of $\psi(0, +)$ is order g smaller than $\psi(d)$. Hence the amount of the leak is small ($\sim g^2$). The same analysis applies to the state $R2$, which is also a quasibound state. Figure 4 shows that the quasibound states survive over a wide range of the parameter E_d.

Let us remark here on the relation between the QBIC and BIC states. Strictly speaking, our quasibound state is not in continuum, because its energy spectrum has an imaginary component (a decay rate). Because of the van Hove singularity, however, this decay rate is extremely small (proportional to g^6, much smaller than the ordinary decay rate $\sim g^2$ estimated by the Fermi golden rule in the nonsingular case). Hence, the QBIC may behave as if it were a bound state even on relatively large time scales. As another remark, while BIC is a true bound state with a real energy spectrum under ideal conditions, since BIC exists only at discrete points with zero measure in parameter space (such as the unperturbed energy E_d), any noise (e.g., thermal noise, incompleteness of the device, etc.) in an actual experimental setup may lead to a small decay rate (i.e., a small imaginary part of the energy spectrum) for the BIC. In this sense the QBIC state will behave essentially as the BIC under actual experimental conditions. On the contrary, since QBIC exists for a wide range of parameter space, it may be easier to prepare QBIC in the experiment.

To summarize, we have found quasibound states in continuum over a wide range of system parameters, which is in striking contrast to the bound state in continuum. The quasibound states emerge in the system with two overlapping eigenvalue continua when at least one of the bands contains a divergent van Hove singularity. For instance, a would-be bound state just below the upper continuum turns out to be a quasibound state in the lower continuum. The simple picture of this mechanism suggests that the quasibound state may be found in various systems including a microwave tube with an atom or molecule [12] and in the scattering of ions and nuclides.

The authors thank Professor Satoshi Tanaka for useful discussions. This work is supported partly by the National Institutes of Natural Sciences undertaking Forming Bases for Interdisciplinary and International Research through Cooperation Across Fields of Study and the NIFS Collaborative Research Program (No. NIFS06KDBT005, No. NIFS06KDAT012, No. NIFS07USNN002, and No. NIFS07KEIN0091) as well as by Grant-in-Aid for Scientific Research (No. 17340115 and No. 17540384) from the Ministry of Education, Culture, Sports, Science and Technology. One of the authors (N. H.) acknowledges support by Core Research for Evolutional Science and Technology (CREST) of Japan Science and Technology Agency. This material is based upon work supported by the National Science Foundation under Grant No. 0611506.

*hnakamura@nifs.ac.jp
†hatano@iis.u-tokyo.ac.jp

[1] J. von Neumann and E. Wigner, Phys. Z. **30**, 465 (1929).
[2] F. H. Stillinger and D. R. Herrick, Phys. Rev. A **11**, 446 (1975).
[3] B. Gazdy, Phys. Lett. A **61**, 89 (1977).
[4] L. Fonda and R. G. Newton, Ann. Phys. (N.Y.) **10**, 490 (1960).
[5] H. Friedrich and D. Wintgen, Phys. Rev. A **31**, 3964 (1985).
[6] F. Capasso, C. Sirtori, J. Faist, D. L. Sivco, S.-N. G. Chu, and A. Y. Cho, Nature (London) **358**, 565 (1992).
[7] P. S. Deo and A. M. Jayannavar, Phys. Rev. B **50**, 11 629 (1994).
[8] G. Ordonez, K. Na, and S. Kim, Phys. Rev. A **73**, 022113 (2006).
[9] A. F. Sadreev, E. N. Bulgakov, and I. Rotter, Phys. Rev. B **73**, 235342 (2006).
[10] E. N. Bulgakov, K. N. Pichugin, A. F. Sadreev, and I. Rotter, JETP Lett. **84**, 430 (2006).
[11] G. D. Mahan, *Many Particle Physics* (Plenum, New York, 1990), 2nd ed., p. 283.
[12] T. Petrosky, C.-O. Ting, and S. Garmon, Phys. Rev. Lett. **94**, 043601 (2005).
[13] S. Tanaka, S. Garmon, and T. Petrosky, Phys. Rev. B **73**, 115340 (2006).
[14] K. Kobayashi, H. Aikawa, A. Sano, S. Katsumoto, and Y. Iye, Phys. Rev. B **70**, 035319 (2004).
[15] I. Maruyama, N. Shibata, and K. Ueda, J. Phys. Soc. Jpn. **73**, 3239 (2004).
[16] K. O. Friedrichs, Commun. Pure Appl. Math. **1**, 361 (1948).
[17] E. C. G. Sudarshan, *Structure of Dynamical Theories*, Brandeis Lectures in Physics (W. A. Benjamin, New York, 1962).
[18] U. Fano, Phys. Rev. **124**, 1866 (1961).
[19] P. W. Anderson, Phys. Rev. **124**, 41 (1961).
[20] N. Hatano, H. Nakamura, K. Sasada, and T. Petrosky, arXiv:0705.1388.